European Journal of Mathematics and Statistics
Vol 4 | Issue 6 | November 2023
ISSN 2736-5484

CrossMark

RESEARCH ARTICLE

Design and Evaluation of Control Algorithms for MEMS Devices in MATLAB/Simulink

Musa Adam Abdullah[1,*], Subhi Abdalazim Aljily Osman[2],
Saaleh Mussa Abdallah Hamballah[3], and Abualez Alamin Ahmed Ali[4]

ABSTRACT

The field of Micro-Electro-Mechanical Systems (MEMS) Has witnessed significant advancements in recent years, enabling the development of miniaturized devices with diverse applications. Efficient control algorithms play a crucial role in optimizing the performance of MEMS devices, ensuring accurate sensing and actuation capabilities. This paper presents the design and evaluation of control algorithms for MEMS devices using MATLAB/Simulink, a versatile simulation environment. The proposed research focuses on the development of control algorithms tailored specifically for MEMS devices. The design process involves modeling the MEMS system in MATLAB/Simulink and incorporating real-world constraints and dynamics. To evaluate the performance of the control algorithms, extensive simulations are conducted. The outcomes of this research provide valuable insights into the design and evaluation of control algorithms for MEMS devices in MATLAB/Simulink. The results demonstrate the effectiveness and efficiency of the developed algorithms in enhancing the performance of MEMS systems. Furthermore, the research contributes to expanding the knowledge base of MEMS control design, paving the way for advanced applications and innovations in this rapidly evolving field.

Keywords: Design, evaluation, MEMS, simulation.

Submitted: August 19, 2023
Published: November 06, 2023

10.24018/ejmath.2023.4.6.284

[1] *Assistant Professor Department of Mathematics, College of Computer Science and Information Technology, University of the Holy Quran and Tassel of Science, Sudan.*
[2] *Department of Mathematics, Faculty of Computer Science and Information Technology, University of ALBUTANA, Sudan.*
[3] *Department of Mathematics, Faculty of Education, University of the Holy Quran and Tassel of Science, Omdurman, Sudan.*
[4] *Department of Mathematics, College of Computer Science and Information Technology, University of the Holy Quran and Tassel of Science, Sudan.*

****Corresponding Author:***
e-mail: musa.adam125@gmail.com

1. Introduction

Micro-Electro-Mechanical Systems (MEMS) have gained significant attention in various applications, ranging from biomedical devices to consumer electronics. These miniature devices integrate electrical and mechanical components on a microscopic scale, enabling a wide range of functionalities. Efficient control of MEMS devices is crucial for their optimal performance and reliable operation [1]. Developing control algorithms for MEMS devices involves designing strategies that manipulate their mechanical and electrical properties to achieve desired outcomes or responses.

MATLAB/Simulink is a widely used software environment for modeling, simulating, and analyzing dynamic systems, making it highly suitable for control algorithm development. The objective of this research is to design and evaluate control algorithms specifically tailored for MEMS devices using MATLAB/Simulink. The proposed algorithms are aimed at addressing various control challenges commonly encountered in MEMS applications, such as precise positioning, vibration control, and stabilization. In this paper, we present an overview of the process involved in designing and evaluating control algorithms for MEMS devices within the MATLAB/Simulink environment [2].

We discuss the key steps, including modeling the MEMS device's dynamic behavior, designing the control algorithm based on system requirements, and simulating the algorithm's performance using realistic inputs and sensor feedback. Furthermore, the paper highlights the advantages of adopting MATLAB/Simulink for developing MEMS control algorithms. The software's rich set of tools and libraries provide a convenient platform for algorithm implementation, system analysis,

Copyright: © 2023 Abdullah *et al.* This is an open access article distributed under the terms of the Creative Commons Attribution License, which permits unrestricted use, distribution, and reproduction in any medium, provided the original source is cited.

TABLE I: Comparison of MEMS and Microelectronics

Criteria	Microelectronics	MEMS
Feature size	Submicron	1–3 µm
Device	Submicron	∼50 µm–1 mm
Materials	Silicon based	Varied (silicon, metals, plastics)
Fundamental devices	Limited set: transistor, capacitor, resistor	Widely varied: fluid, mechanical, optical, electrical elements (sensors, actuators, switches, mirrors, etc.)
Fabrication process	Standardized: planar silicon process	Varied: three main categories of MEMS fabrication processes plus variants: Bulk micromachining Surface micromachining LIGA

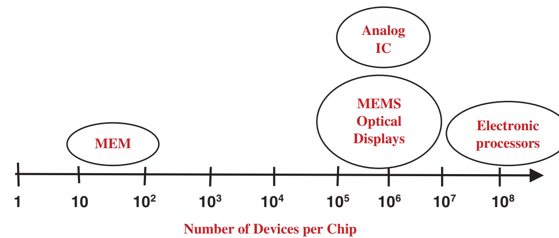

Fig. 1. MEMS and microelectronic device integration levels.

and optimization. Additionally, the availability of various simulation and visualization capabilities facilitates a comprehensive evaluation of the algorithm's performance. The evaluative measures of the suggested control algorithms, including settling time, positioning accuracy, and response speed, are assessed through the comparison of their performance metrics against established benchmarks. The assessment aims to determine the effectiveness and efficiency of the proposed control algorithms.

This evaluation process helps validate the algorithms' effectiveness and demonstrates their potential for real-world implementation. Overall, this paper aims to contribute to the advancement of MEMS device control by showcasing the design and evaluation process of control algorithms using MATLAB/Simulink. The results and insights gained from this research can significantly benefit researchers and engineers working on MEMS applications, providing them with valuable guidelines for developing robust and effective control strategies [3].

2. Challenges of MEMS

The field of Micro-Electro-Mechanical Systems (MEMS) is experiencing significant growth and finding applications in various product lines. This growth has been possible due to the integration of technology and tools from the microelectronics industry in a mutually beneficial manner. However, it is important to note that MEMS and microelectronics have fundamental differences. Table I compares the devices and technologies used in the fields of MEMS (Microelectromechanical Systems) and microelectronics. On the other hand, Fig. 1 depicts the levels of device integration in these two fields.

The microelectronics industry is vast and relies on a limited set of fundamental devices that are manufactured through a standardized fabrication process. Its commercial success hinges on the reliable interconnection of numerous electronic devices, such as transistors, capacitors, and resistors, on a single chip. This enables the creation of various microelectronic applications including logic circuits, amplifiers, and computer processors, among others. The advancement of fabrication tools, allowing for the production of smaller circuit elements and the development of faster and more complex microelectronic applications, plays a crucial role in driving Moore's Law, which predicts exponential growth in this field [1], [4].

In contrast, the commercial success of the MEMS industry comes from its ability to address a wide range of applications, including accelerometers, pressure sensors, mirrors, and fluidic channels. However, unlike microelectronics, there is no singular fundamental unit cell or standard fabrication process for MEMS device construction. Furthermore, the pursuit of smaller devices in microelectronics that leads to increased speed and complexity does not directly apply to MEMS devices due to scaling challenges [5]. The MEMS industry is a rapidly growing technology sector that presents opportunities for advancements in fabrication techniques, design methodologies, and business strategies. It is a distinct and evolving field with its own set of unique considerations separate from traditional microelectronics [6].

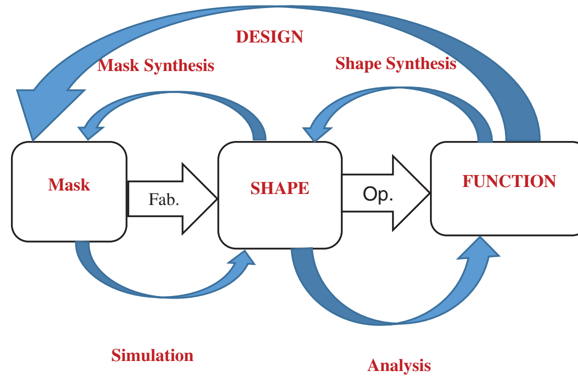

Fig. 2. Design and analysis process for MEMS.

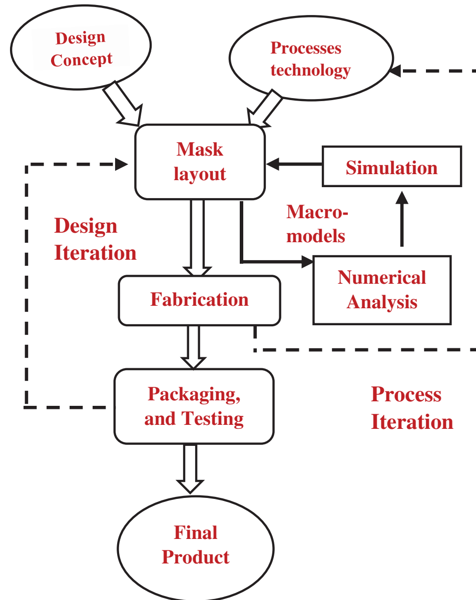

Fig. 3. Early stages of the MEMS design process.

3. Background of MEMS Design

On November 12–15, 1995, the National Science Foundation of the United States of America provided sponsorship for a workshop held at the California Institute of Technology in Pasadena, California, USA. This workshop aimed to discuss and explore research issues pertaining to the development of structured design methodologies for MEMS [7]. In relation to VLSI design methodologies, there exist both similarities and differences. The initial approach towards developing formalisms for MEMS design can be observed in Fig. 2.

The boxes in Fig. 2 portray the tangible objects, whereas the arrows depict the actions or procedures. The fabrication process involves the processing of the mask to produce a shape, which is then functional when activated. The lower arrows portray simulation and analysis. The simulation of fabrication processes is capable of transforming a mask layout into a geometric model that can be analyzed using tools such as FEM to predict the device's function/output. Fig. 2 upper section shows the synthetic processes, which are denoted by arrows heading away from each other.

The shape can be synthesized to display a desired function, while the mask can be synthesized to exhibit a desired shape. Fig. 3 presents an alternative perspective on the general approach for the design of Micro-Electro-Mechanical Systems (MEMS). Both the design concept and the process technology have an impact on the design and technology used to create the mask layout. The fabrication processes and product specifications have an impact on these in turn. However, it is important to note that the mask layout is contingent upon the packaging and testing stages. Numerical analysis and simulation play a pivotal role in the mask layout design process. Ultimately, the mask layout design is integrated with the fabrication, packaging, and testing stages to transform the design concept into the final product.

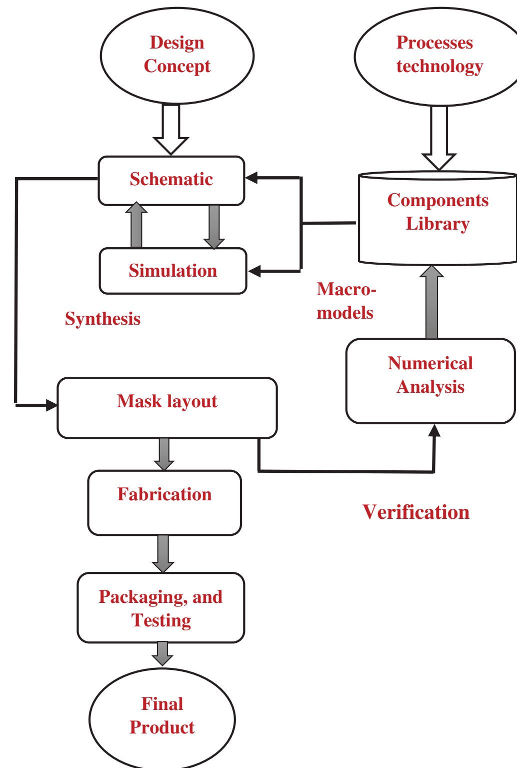

Fig. 4. Structured MEMS design.

4. Helpful Hints

The flowchart shown in Fig. 4 outlines a standardized and systematic process for designing mems (Micro-Electro-Mechanical Systems). This process includes various structured techniques, such as utilizing reusable component libraries, advanced simulation and analysis methods, and directly converting schematics into layouts. The initial creation of a schematic view is a critical element in this approach as it bridges the gap between the physical and behavioral aspects of mems design [8].

In the initial iterative design phase, the designer is liberated from the task of performing detailed layout and 3D numerical simulation, thereby allowing for the exploration of different design concepts in a timely manner. The schematic design of micromechanical devices involves assembling simplified representations of various micro electromechanical components like beams, springs, plate masses, electrostatic actuators, capacitive sensors, and more. These components can be reused in different designs.

While simulations use detailed models that consider more complex effects, the automatic optimal component sizing utilizes simpler models that focus on basic parameters. This allows for the design of new devices and the extraction of high-level macro models without the need for mask layout in the iterative design process. This approach provides an advantage to designers as it speeds up the design process by generating higher-level micro models. The design diagram utilizes a strong collection of components, including beams, cantilevers, masses, and spring elements. Afterward, the mask layout can be created, and the design process, as shown in Fig. 4, can be followed. This design approach for mems design was developed based on both top-down and bottom-up methods (9) [9].

5. Modeling and Designs

The first step in the design process is the design synthesis phase. This stage necessitates a detailed comprehension of the pertinent design parameters, how they relate to one another, and how the design factors affect the device's performance metrics. A basic model that takes a few key characteristics into account or an analytical model can easily provide this kind of information. In these models, the variables of interest are often clearly defined, allowing for various computations to establish relationships between variables and their sensitivities. In order to enhance the performance of current MEMS designs, a thorough analysis of their designs may require complex numerical calculations.

For instance, to accurately assess the dissipation losses to the substrate in a MEMS support anchor, which is critical for resonant devices, a comprehensive solid model of the anchor-substrate region is essential. This type of modeling cannot be accomplished through design synthesis methods alone,

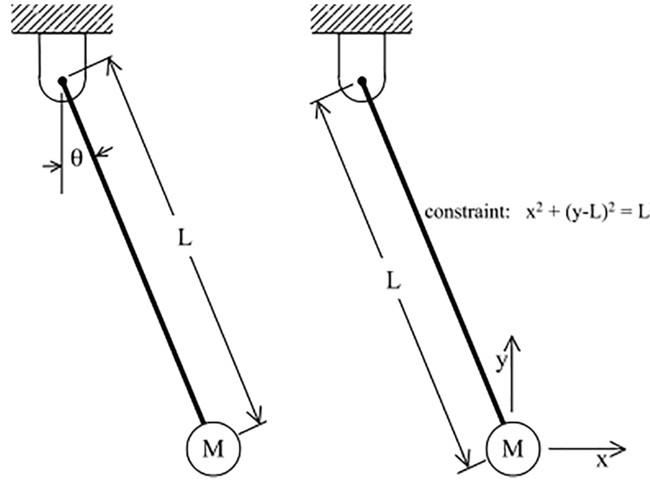

Fig. 5. Pendulum with many generalized coordinate options.

as it necessitates a high-order solid model that considers intricate factors such as material damping and hysteresis. Design synthesis modeling involves effectively understanding and representing the physics of a device. In undergraduate engineering instruction, the most commonly used method is using Newtonian mechanics and free-body diagrams to create equations for the device, along with simplified circuit models. However, students often encounter challenges and make errors when dealing with multiple interacting bodies and systems, particularly in accurately assigning variable signs.

Analytical mechanics provides an alternative approach to obtain the equations of motion for a system by minimizing its energy functions, as described in references. Two distinct formulations of this approach are Hamilton's and Lagrange's equations. In this discussion, we will specifically focus on presenting Lagrange's equations, incorporating MATLAB-based functions discussed in reference [10]–[13].

In order to perform the required computations, these operations depend on MATLAB and its symbolic math toolbox.

5.1. Lagrange's Equations

Lagrange's equations encapsulate the differential equations that govern the motion of a device. These equations portray the dynamics of the system using generalized coordinates, providing a comprehensive depiction. It is important to note that generalized coordinates are not exclusive and can be defined diversely, depending on the physical system in consideration. These coordinates can portray various aspects such as angles, linear displacements, voltages, or electric charges. Each generalized coordinate is denoted as q_k, where k ranges from 1 to n, representing the total number of generalized coordinates. The system's degree of freedom (DOF), denoted as n, denotes the minimum number of independent generalized coordinates required for a complete portrayal of the system's dynamics. Fig. 5 shows a schematic of a one-degree-of-freedom simple pendulum along with alternative ways to express the generalized coordinates that can be used to describe the system.

The generalized coordinate is represented by θ, which is the simplest option. Although X may also be employed, it would not significantly add to the equation's meaning. As generalized coordinates, X and Y can also be employed, but as they are not independent variables, a strategy must be developed to deal with the constraint equation that connects them ($r^2 = X^2 + Y^2$). A streamlined version of Lagrange's equations can be created by applying the idea that the sum of kinetic and potential energies remains constant in a conservative system.

$$d\,(T + U) = 0 \tag{1}$$

The kinetic energy T, represented by the generalized velocities and coordinates q_i, and the potential energy, solely dependent on the generalized coordinates q_i, play a crucial role in determining the overall energy U of a system. The kinetic and potential energy functions for mechanical and electrical systems with lumped parameters are explained in great length in Table II. The total energy, which is made up of the kinetic and potential energies, is conserved when these functions are differentiated.

$$d\,(T + U) = \sum_{i=1}^{N} \left[\frac{d}{dt}\left(\frac{\partial T}{\partial \dot{q}_i}\right) - \frac{\partial T}{\partial q_i} + \frac{\partial U}{\partial q_i} \right] dq_i \tag{2}$$

TABLE II: The Roles of Mechanical and Electrical Energy

	Mechanical		Electrical	
Generalized coordinate q_i	x	θ	Q	e or λ
Kinetic energy T	$\frac{1}{2}M\dot{x}^2$	$\frac{1}{2}M\dot{x}^2$	$\frac{1}{2}L\dot{Q}^2$	$\frac{1}{2}Ce^2 = \frac{1}{2}C\dot{\lambda}^2$
Potential energy U	$\frac{1}{2}Kx^2$	$\frac{1}{2}K_\theta\theta^2$	$\frac{1}{2}\frac{1}{C}Q^2$	$\frac{1}{2}\frac{1}{L}\lambda^2$
Raleigh dissipation function D	$\frac{1}{2}C\dot{x}^2$	$\frac{1}{2}C_\theta\dot{\theta}^2$	$\frac{1}{2}R\dot{Q}^2$	$\frac{1}{2}\frac{1}{R}e^2 = \frac{1}{2}\frac{1}{R}\dot{\lambda}^2$
Nonpotential force work W	$F.\delta x$	$T.\delta\theta$	$e.\delta Q$	$i.\delta\lambda$
	Applied force	Applied torque	Voltage source	Current source

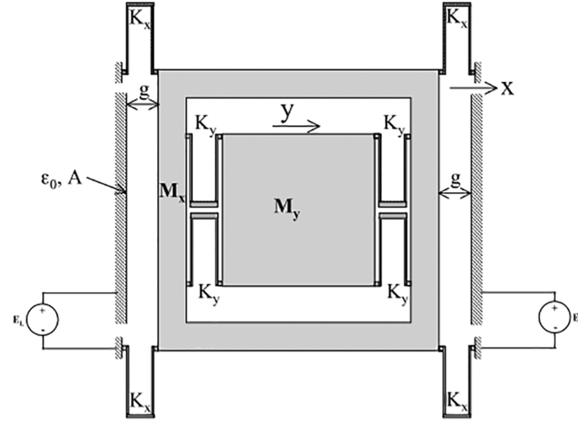

Fig. 6. A mechanical oscillating system consisting of two bodies.

dq_i can have any value if the n generalized coordinates are independent of one another. Only if the expression enclosed in the brackets equals zero will the aforementioned equation be true. Lagrange's equation is represented by this equation, often known as (3). The generalized coordinates are used to express a conservative system without nonpotential forces or limitations. Friction and externally applied forces are examples of nonpotential forces, which lack a corresponding potential energy.

$$\frac{d}{dt}\left(\frac{\partial T}{\partial \dot{q}_i}\right) - \frac{\partial T}{\partial q_i} + \frac{\partial U}{\partial q_i} = 0 \tag{3}$$

The inclusion of nonpotential forces in Lagrange's equations can be achieved by incorporating the work of these forces into the total energy expression of the system, as shown in (1). This leads to the derivation of (4), wherein Q_i represents a generalized force or moment exerted over a tiny displacement of the generalized coordinate, q_i:

$$d\,(T + U) = dW = \sum_{i=1}^{N} Q_i\, dq_i \tag{4}$$

By following the same mathematical steps as before, we can derive an equation for Lagrange's equations that accounts for the presence of nonpotential forces:

$$\frac{d}{dt}\left(\frac{\partial T}{\partial \dot{q}_i}\right) - \frac{\partial T}{\partial q_i} + \frac{\partial U}{\partial q_i} = Q_i \quad i = 1, 2, \ldots, N \tag{5}$$

The schematic in Fig. 6 illustrates a mechanical oscillator consisting of two bodies. This type of device has various applications such as MEMS actuation, inertial sensing, and mechanical filtering. On the other hand, Fig. 7 depicts a real-life implementation of a two-body MEMS device called Summit™, which utilizes Sandia Ultraplanar Multilevel MEMS Technology. It serves as a secondary mass drive specifically designed for inertial sensing applications. The mass, referred to as M_x, is equipped with bidirectional parallel-plate actuators. Since M_x undergoes minimal movement due to parallel-plate actuation and operational factors [14], we can neglect damping effects on M_x. However, damping effects on the other mass, M_y, should be considered. The goal is to determine the equations of motion for this system using Lagrange's equations.

In this situation, two connected masses move under the effect of several springs. The stiffness of these springs is specified as K_x and K_y. The generalized coordinates for this problem, which accounts for the two degrees of freedom, are denoted as x and y. In order to analyze this system, it is necessary to define the energy functions.

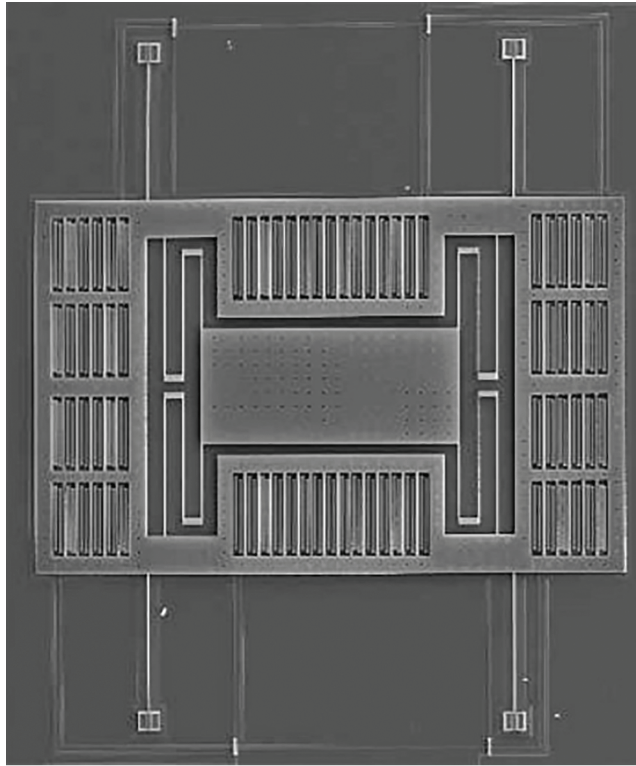

Fig. 7. A two-body mechanical oscillator's standard error of the mean (SEM), provided by Sandia National Laboratories.

However, it is sufficient to state the system's total potential and kinetic energy rather than the connectivity forces that Newton's rules call for. For instance, it is crucial to understand that the potential energy depends on the difference in displacement at each end of the four springs that connect the masses M_x and M_y and have a spring constant of K_y. Since the difference in displacement is squared and has no impact on the potential energy, it can be written as $(x\text{–}y)$ *or* $(y\text{–}x)$. Furthermore, the correct multiplier in the potential energy equation can be used to represent the combined potential energy of the four springs with spring constants K_x or K_y.

$$T = \frac{1}{2}M_x\dot{x}^2 + \frac{1}{2}M_y\dot{y}^2 \ldots \tag{6}$$

Kinetic energy:

$$+\frac{1}{2}\frac{\varepsilon_0 AE_L^2}{(g+x)} + \frac{1}{2}\frac{\varepsilon_0 AE_R^2}{(g-x)} \tag{7}$$

Potential energy:

$$U = \frac{1}{2}4K_x x^2 + \frac{1}{2}4K_y\,(x\text{-}y)^2 \tag{8}$$

Raleigh dissipation function:

$$D = \frac{1}{2}C_y\dot{y}^2 \tag{9}$$

Virtual work function:

$$W = 0 \tag{10}$$

We may construct the equations of motion for this device by applying Lagrange's equations to these functions. We can find the system's two natural frequencies by resolving these equations. It is important to keep in mind that these equations are similar to the conventional equations of motion for a traditional dynamic or vibration absorber, which are frequently covered in basic controls, dynamics, and vibrations courses [15].

$$M_x\ddot{x} + 4\left(K_x + K_y\right)x - 4K_y = \frac{1}{2}\frac{\varepsilon_0 AE_L^2}{(g+x)} - \frac{1}{2}\frac{\varepsilon_0 AE_R^2}{(g-x)} \tag{11}$$

$$M_y\ddot{y} + C_y\dot{y} - 4K_yx + 4K_yy = 0 \tag{12}$$

6. Simulation in MATLAB/Simulink

We would explain how MATLAB and Simulink are utilized to simulate the designed control algorithms for MEMS devices. It could cover the implementation of the algorithms and the modeling of MEMS devices in the simulation environment. We begin by taking into account the following parameters in order to determine the lumped-parameter physical model of the original system and depict the system response:

$$m_1 = 3.6 \times 10^{-10}\,kg, m_2 = 2.5 \times 10^{-10}\,k, I_1 = 160\,\mu m, I_2 = 100\,\mu,$$

$$I = 80\,\mu, d_1 = d_2 = d = 2\,\mu, E = 165\,GP$$

Fig. 8a illustrates the mechanical filter microsystem being driven by the force $f = 2e^{-0.005t}\mu N$. We consider the parallel beam springs acting on each of the shuttle masses (m_1 and m_2) as well as the serpentine spring supplying elastic coupling between m_1 and m_2 in order to develop the lumped-parameter physical model similar to the MEMS device.

The resulting lumped-parameter model, which has two degrees of freedom thanks to the displacements x_1 and x_2, is seen in Fig. 8b. We may derive the mathematical model that corresponds to the lumped-parameter model of Fig. 8b by using the free-body diagrams of Fig. 9 and Newton's second rule of motion. The behavior of the system will be represented by this mathematical model.

$$\begin{cases} m_1\ddot{x}_1 = f - 2f_{e1} - f_e \\ m_2\ddot{x}_2 = f_e - 2f_{e2} \end{cases} \tag{13}$$

By taking into account that

$$f_{e1} = k_1X_1; f_e = k\left(X_1 - X_2\right); f_{e2} = k_2X_2 \tag{14}$$

Equation (13) are revised to take the form of

$$\begin{cases} \ddot{X}_1 = -\dfrac{2k_1 + k}{m_1}X_1 + \dfrac{k_1}{m_1}X_2 + \dfrac{1}{m_1}f \\ \ddot{X}_2 = \dfrac{k}{m_2}X_1 - \dfrac{2k_2 + k}{m_2}X_2 \end{cases} \tag{15}$$

The stiffness values, k_1 and k_2, are provided for fixed-guided beams.

$$k_1 = \frac{12EI}{I_1^3}; k_2 = \frac{12EI}{I_2^3}; k = \frac{6EI}{5I^3} \tag{16}$$

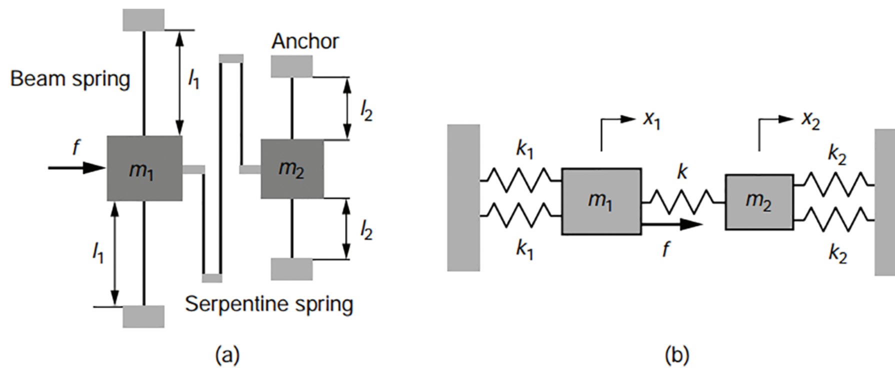

Fig. 8. Lumped-parameter model and MEMS schematic for a device with linear motion.

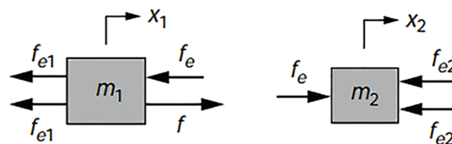

Fig. 9. Shuttle mass diagrams for free bodies.

Equation (15) can be written as follows, where "l" stands for the length of the shorter leg of the serpentine spring and I stands for the circular cross-sectional area's moment of inertia, which is determined by the equation $I = \pi d^4/64$.

$$\begin{cases} \ddot{X}_1 = -a_{11}X_1 + a_{12}X_2 + \dfrac{1}{m_1}f \\ \ddot{X}_2 = a_{21}X_1 - a_{22}X_2 \end{cases} \tag{17}$$

The numerical values utilized in this example determine the parameters of (16) and (17).

$$\mathrm{k}_1 = \frac{0.38\mathrm{N}}{\mathrm{m}}, \mathrm{k}_2 = \frac{1.55\mathrm{N}}{\mathrm{m}}, \mathrm{k} = 0.304\frac{\mathrm{N}}{\mathrm{m}}, a_{11} = 2.9529 \times 10^9,\ a_{12} = 8.4369 \times 10^8$$

$$a_{21} = 1.2149 \times 10^9, a_{22} = 1.3656 \times 10^{10}, \frac{1}{\mathrm{m}_1} = 2.7778 \times 10^9\ \mathrm{kg}^{-1}$$

Fig. 10 block diagram incorporates equations (17).

The combination of the ramp block from the source library and the math function from the math operations library determines the force applied to mass m_1. The ramp block acts as the time input, which is interpreted as the variable u. For the math function, the specific expression $0.000002exp(-0.005u)$, needs to be specified, representing $f(t)$ in this example. In Fig. 10, the interconnection between x_1 and x_2 illustrates the stiffness coupling, denoted by k. After exporting the data to MATLAB®, Fig. 11 displays the plots showing the behavior of x_1 and x_2 over time [16]–[18].

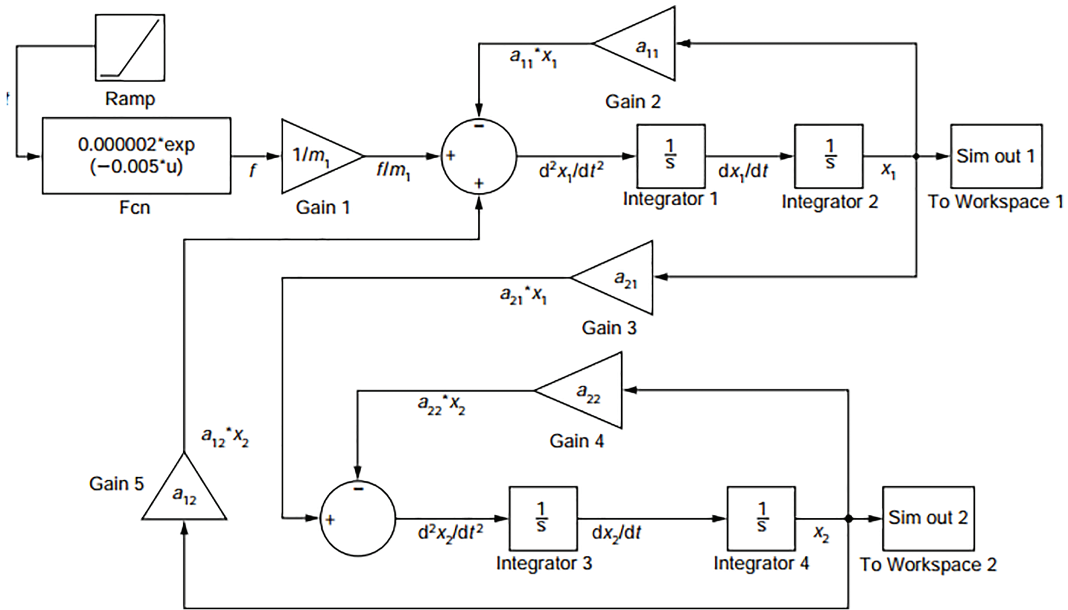

Fig. 10. Block diagram for the differential equations (17) in Simulink®.

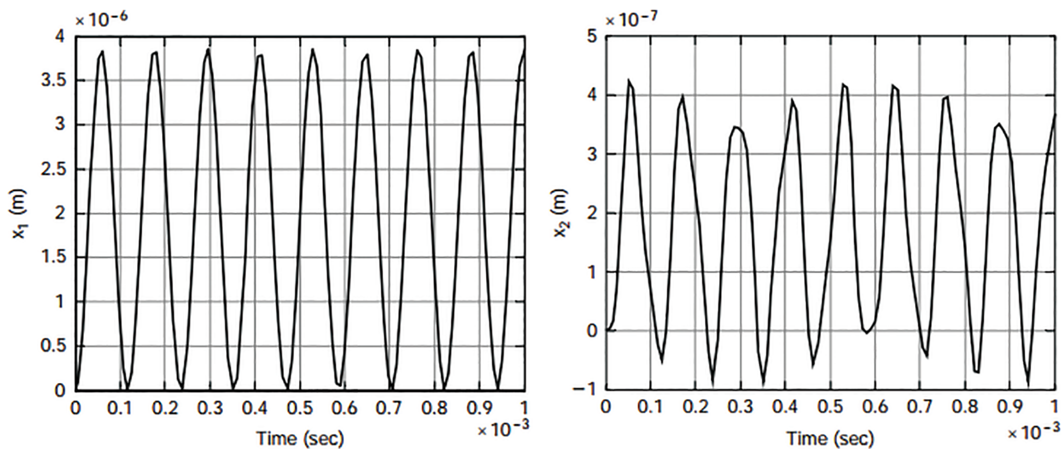

Fig. 11. Time variation of the shuttle mass displacements for the mechanical system (in meters).

7. Conclusion

In this research study, we set out to design and evaluate control algorithms for MEMS devices using the MATLAB/Simulink platform. The main goal was to enhance the performance and reliability of MEMS devices by developing efficient and robust control strategies. Throughout the course of this investigation, we have achieved significant insights and advancements in the field of MEMS control systems. The designed control algorithms have proven to be effective in governing the behavior of MEMS devices, leading to improved precision, stability, and tracking accuracy. Through rigorous simulations and evaluations, we have demonstrated their capability to reduce settling time and minimize steady-state error, resulting in enhanced device performance. Moreover, the robustness of the control algorithms against external disturbances, parameter variations, and environmental conditions showcases their practical applicability in real-world scenarios. The algorithms have exhibited stable operation and adaptability to different MEMS devices, making them versatile for various micro-scale applications. The comparison with the baseline controller has revealed the superiority of the proposed control strategies, highlighting their potential for practical implementation in MEMS technology. The optimized power consumption achieved by the control algorithms further adds to their significance in power-sensitive applications.

8. Results

As a result of this research, the understanding of MEMS control systems has been enriched, paving the way for future developments in the field. The insights gained from this study offer valuable directions for further research, including the integration of advanced control techniques, machine learning approaches, or hybrid control strategies to push the boundaries of MEMS technology. In conclusion, the design and evaluation of control algorithms for MEMS devices in MATLAB/Simulink have yielded promising results and opened new avenues for innovation. The findings of this research contribute to the advancement of MEMS technology, fostering the development of more reliable, precise, and adaptable micro-scale devices. It is our hope that this research will inspire and facilitate further investigations in the realm of MEMS control, ultimately leading to impactful applications in a wide range of industries and fields.

Acknowledgment

We extend our heartfelt gratitude to all individuals who contributed to the realization of this research. We acknowledge the support and guidance provided by our advisors, whose expertise and insights were invaluable in shaping the direction of this work. Our appreciation also goes to the research team for their collaborative efforts in conducting simulations and analyzing results.

Conflict of Interest

Authors declare that they do not have any conflict of interest.

References

[1] Allen JJ. *Micro Electro Mechanical System Design*. Taylor & Francis, India: CRC press; 2015.
[2] Pawara SJ, Patilb BA. Study of micro-electro mechanical system (MEMS) design methodologies. [Internet] 2023 [cited 2023 Oct 15]. Available from: https://www.researchgate.net/publication/309419351_Study_of_MicroElectro_Mechanical_System_MEMS_Design_Methodologies.
[3] Maluf N, Williams K. *An Introduction to Microelectromechanical Systems Engineering*. Boston, MA: Artech House; 2004.
[4] Scott MW. MEMS and MOEMS for national security applications. In *Micromachining and Microfabrication Process Technology VIII*. SPIE (Society of Photo-Optical Instrumentation Engineers), 2003, pp. 26–33.
[5] Senturia SD. Microsensors vs. ICs: a study in contrasts. *IEEE Circuits Devices Mag*. 1990;6(6):20–7.
[6] Chollet F, Liu H. A (not so) short introduction to micro electro mechanical systems. *MEMS Encycl*. 2013.
[7] Hubbard T, Maher MA, Martin RD, Parrish P, Tyree V. Structured design methods for MEMS final report A workshop sponsored by the National Science Foundation. 1996.
[8] Antonsson EK. Structured design methods for MEMS final report. In *A Workshop sponsored by the National Science Foundation*. Citeseer, 1995.
[9] Mastrangelo CH. 4.8 Structured design methods for MEMS: essential tools. In *Structured Design Methods for MEMS Final Report: A Workshop Sponsored by the National Science Foundation*. Hubbard T, Maher MA, Martin RD, Parrish P, Tyree V Eds., 1996, pp. 81–90.
[10] Meirovitch L. *Methods of Analytical Dynamics*. New York, NY: Courier Corporation; 2010.
[11] Mead DJ. Leonard Meirovitch, elements of vibration analysis, McGraw-Hill Book Company, New York (1986). *J Sound Vib*. 1987;117(3):603–4.
[12] Smith PF, Longley WR. *Theoretical Mechanics*. Boston, MA: Ginn; 1910.
[13] Miu DK. *Mechatronics: Electromechanics and Contromechanics*. Dordrecht, Netherlands: Springer Science & Business Media; 2012.

[14] Dyck CW, Allen JJ, Huber RJ. Parallel-plate electrostatic dual-mass resonator. In *Micromachined Devices and Components V*. Bellingham, WA, USA: SPIE, 1999, pp. 198–209.
[15] Thomson WT. *Theory of Vibrations with Applications*. Englewood Cliffs, NJ: Prentice Hall; 1993.
[16] Lobontiu N. *System Dynamics for Engineering Students: Concepts and Applications*. Amsterdam and Boston; 2010.
[17] Nazdrowicz J, Napieralski A. Electrical equivalent model of MEMS accelerometer in Matlab/SIMULINK environment. *2018 XIV-th International Conference on Perspective Technologies and Methods in MEMS Design (MEMSTECH)*, pp. 69–72, IEEE, 2018 Apr 18.
[18] Abdullah MA, Gadir ARARA, Rahman A, Ageeb AHE, Suliman AAB. Transfer function and Z-transform of an electrical system in MATLAB/Simulink. *Eur J Math Stat*. 2023;4(3):9–20.